UCLan
University of Central Lancashire

Article

Microbial Reduction of U(VI) under Alkaline Conditions: Implications for Radioactive Waste Geodisposal

Williamson, Adam J., Morris, Katherine, Law, Gareth T. W., Rizoulis, Athanasios, Charnock, John M. and Lloyd, Jonathan R.

Available at http://clok.uclan.ac.uk/17298/

It is advisable to refer to the publisher's version if you intend to cite from the work.
http://dx.doi.org/10.1021/es5017125

For more information about UCLan's research in this area go to
http://www.uclan.ac.uk/researchgroups/ and search for <name of research Group>.

For information about Research generally at UCLan please go to
http://www.uclan.ac.uk/research/

CLoK
Central Lancashire online Knowledge
www.clok.uclan.ac.uk

CLoK
University of Central Lancashire's Institutional Repository

# Microbial Reduction of U(VI) under Alkaline Conditions: Implications for Radioactive Waste Geodisposal

Adam J. Williamson,[†] Katherine Morris,[†] Gareth T. W. Law,[‡] Athanasios Rizoulis,[†] John M. Charnock,[†] and Jonathan R. Lloyd*,[†]

[†]Research Centre for Radwaste Disposal and Williamson Research Centre for Molecular Environmental Science, School of Earth, Atmospheric and Environmental Sciences, The University of Manchester, Manchester, M13 9PL, United Kingdom

[‡]Centre for Radiochemistry Research and Research Centre for Radwaste Disposal, School of Chemistry, The University of Manchester, Manchester, M13 9PL, United Kingdom

Ⓢ Supporting Information

ABSTRACT: Although there is consensus that microorganisms significantly influence uranium speciation and mobility in the subsurface under circumneutral conditions, microbiologically mediated U(VI) redox cycling under alkaline conditions relevant to the geological disposal of cementitious intermediate level radioactive waste, remains unexplored. Here, we describe microcosm experiments that investigate the biogeochemical fate of U(VI) at pH 10−10.5, using sediments from a legacy lime working site, stimulated with an added electron donor, and incubated in the presence and absence of added Fe(III) as ferrihydrite. In systems without added Fe(III), partial U(VI) reduction occurred, forming a U(IV)-bearing non-uraninite phase which underwent reoxidation in the presence of air (O_2) and to some extent nitrate. By contrast, in the presence of added Fe(III), U(VI) was first removed from solution by sorption to the Fe(III) mineral, followed by bioreduction and (bio)magnetite formation coupled to formation of a complex U(IV)-bearing phase with uraninite present, which also underwent air (O_2) and partial nitrate reoxidation. 16S rRNA gene pyrosequencing showed that Gram-positive bacteria affiliated with the *Firmicutes* and *Bacteroidetes* dominated in the post-reduction sediments. These data provide the first insights into uranium biogeochemistry at high pH and have significant implications for the long-term fate of uranium in geological disposal in both engineered barrier systems and the alkaline, chemically disturbed geosphere.
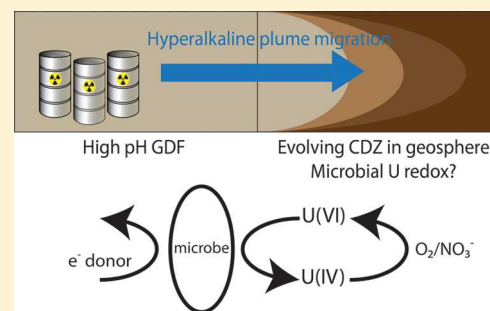
INTRODUCTION

Over the last 50+ years, civilian and military nuclear programs have led to a substantial legacy of intermediate level radioactive wastes, which typically will contain uranium as the most significant radionuclide by mass. In the U.K., Government policy is that these materials will be disposed of in a deep Geological Disposal Facility (GDF), and this position is comparable in many other countries.[1] The environmental behavior of uranium at circumneutral pH is controlled by a combination of complexation, precipitation, redox, and adsorption processes. Under oxidizing conditions, U(VI) predominates as the uranyl ion (UO_2^{2+}), which is relatively soluble as anionic U(VI) carbonate species (e.g., $[UO_2(CO_3)_2]^{2-}_{(aq)}$).[2] It is important to note that U(VI) is also able to interact with sediments and minerals such as ferrihydrite via sorption and/or incorporation and controlled by groundwater chemistry and sediment mineralogy. Under reducing conditions, poorly soluble U(IV) species dominate. The differences in solubility between relatively soluble U(VI) and poorly soluble U(IV) have led to a substantial body of work examining the behavior of U(VI) when microbially mediated reduction is promoted using biostimulation approaches.[3−5] Biostimulation involves the addition of an electron donor such as acetate to the subsurface, which promotes the development of anoxia and precipitation of U(IV). Under biostimulation conditions at neutral pH, both microbially mediated and abiotic U(VI) reduction mechanisms are reported.[6−8] Here, the development of metal- and sulfate-reducing conditions is important, with enzymatic reduction of U(VI) likely to dominate, and both soluble and sorbed U(VI) susceptible to bioreduction.[3,5] Most studies have focused on systems where U(IV) forms uraninite-like phases,[4,5] although more recent work suggests that "non-uraninite" U(IV) bioreduction end products can also form in selected pure culture experiments and natural and engineered sediment systems.[8,9] The non-uraninite U(IV) is thought to be polymeric and coordinated to carboxyl and/or phosphoryl groups on biomass.[8−10] The reoxidation behavior of U(IV) species has also been reasonably well studied under circumneutral conditions, with microcosm experiments showing fast reoxidation, but with column and field observations suggesting

slower reoxidation rates,[11,12] and with Ca(II) and Mn(II) also thought to influence long-term stability of U(IV).[13,14]

Understanding the biogeochemical cycling of uranium is key to predicting its speciation and fate in the shallow subsurface; however, there have been few studies focused on radionuclide biogeochemistry under alkaline conditions relevant to geological disposal where cementitious materials will be used. For example, in many geodisposal concepts, intermediate level wastes (ILW) will be grouted in steel drums and cement will be used for engineering or backfill purposes.[1,15] After ILW disposal, groundwater ingress through the engineered facility is expected. This will result in both an alkaline environment within the engineered barrier system and an alkaline groundwater plume that will move into the surrounding host rock. This will form a persistent, high pH (pH >13–10), chemically disturbed zone that will evolve over geological time scales.[16] The potential for microbial processes stimulated by electron donors (e.g., a variety of organics including, for example, cellulose in the ILW, and cellulose degradation products including organic acids) released into the deep subsurface from the GDF, and associated biogeochemical processes, including metal reduction, is being increasingly recognized.[17−20] This work addresses the paucity of data surrounding such potential processes, focusing on uranium redox cycling in a high pH, biogeochemically active system where U(VI) is predicted to have significant thermodynamic stability.[21] We have used model sediments from an alkaline legacy lime workings site in Buxton, U.K., to characterize the impact of microbial processes on the biogeochemistry of uranium and associated mineralogical phases at pH 10−10.5. Two model systems have been used. In the first, a waste-margin sediment was used to explore the biogeochemical fate of U(VI) in carbonate dominated, alkaline systems, representative of those which are expected to form in the deep disposal of cementitious intermediate waste. In the second, the same sediment was enriched with Fe(III) (as ferrihydrite) to address the impact of stimulated microbial Fe(III) reduction on the behavior of uranium under these conditions. This is important, as iron will be a significant component of ILW (within the waste itself and as engineering components such as rock bolts and steel and their corrosion products) and the wider GDF environment, and Fe(III) reduction is a potential control on uranium solubility. Anthraquinone-2,6- disulfonate (AQDS), an extracellular electron shuttle and humic analogue, was also added to key bioreduction experiments to further explore the mechanisms of U(VI)- and Fe(III)-reduction in these high pH systems where metal solubility is expected to be low. Subsequent experiments examined reoxidation scenarios to assess the potential impact of reaction with oxidants such as nitrate in the waste forms,[22] and the potential for ingress of oxygenated groundwater.[23]

■ MATERIALS AND METHODS

Sediment Collection and Storage. Near surface sediment was collected at the waste margins of the legacy lime workings ponds of an old lime working site in Buxton, U.K. to approximately 10 cm depth.[18] This is an alkaline impacted site where CaO has been weathered over several decades, so that the indigenous microbial population is well developed.[18] Sediments and surface waters (pH 11.8) were transferred into sterile containers and stored at 4 °C in darkness prior to use. Experiments were started within one month of sampling.

Uranium Bioreduction Microcosm Experiments. To determine the fate of U(VI) under anoxic, alkaline conditions,

microcosms were prepared in triplicate; sediments were slurried with 100 g dry sediment L^{-1} of pH 11.8 surface waters, with the initial pH adjusted to 10−10.5 with 1 M HCl. In these model systems, anaerobic microbial processes were stimulated with the addition of 10 mM sodium lactate and 1 g L^{-1} yeast extract similar to recent work.[17,18] Two systems were established: a Buxton sediment and surface water incubation with *no added Fe(III)*, and an experiment *with added Fe(III)*. Here, a 30 mM suspension of nanoscale ferrihydrite,[24] which is well-known to be biologically available,[25] was added. Two additional experiments were established with a soluble electron shuttle added to explore the role of extracellular Fe(III) and U(VI) bioreduction. Here, 100 μM of AQDS was added to microcosms with and without added Fe(III). Uranium from a 42 mM U(VI) in 0.001 M HCl stock was then spiked into all microcosms and experimental controls to a final concentration of 0.42 mM. The bottles were then crimp sealed with thick butyl rubber stoppers and incubated at 20 °C in the dark at pH 10−10.5. Sample manipulations were performed using aseptic technique under anoxic conditions as appropriate. During incubation, the pH of the microcosms dropped during the first fortnight of the experiment, and the pH was then readjusted to pH 10−10.5 using deoxygenated, sterile 2 M NaOH as necessary. Bioreduction experiments were sampled periodically to monitor for biogeochemical changes, and after 210 days samples were removed and stored under anoxic conditions at −80 °C for microbiological (DNA) and X-ray Absorption Spectroscopy (XAS) analysis.

Uranium Reoxidation Experiments. For air (O_2) reoxidation experiments, microbially reduced sediments were transferred into sterile, conical flasks (solid/solution ratio of 1:10) on an orbital shaker at 125 rpm at 20 °C. For nitrate reoxidation experiments, microbially reduced sediment microcosms were amended with $NaNO_3$ to a final concentration of 30 mM nitrate. Reoxidation experiments were sampled periodically to monitor for biogeochemical changes and after 14 days, samples were removed and stored under anoxic conditions at −80 °C for microbiological (DNA) and XAS analysis.

Geochemical Analyses. Sample slurries were analyzed for pH and E_h using a calibrated Denver Instrument Digital Meter and electrodes. To assess the bulk Fe-content of the sediment, aqua-regia digests were performed (Supporting Information, SI). Biogenic Fe(II) and total bioavailable Fe were assessed by 0.5 N HCl extraction via the ferrozine colorimetric assay on a subsample of sediment slurry.[25] Samples were then centrifuged (5 min at 10 500g) and the supernatant was analyzed for total U using an ICP-MS (Agilent 7500cx). In addition, in selected samples, a colorimetric assay for U(VI) was used to assess U speciation in solution.[26,27] Inorganic anions (NO_3^-, NO_2^-, and SO_4^{2-}) were analyzed using a Dionex DX120 ion chromatograph. Colorimetric assays were performed on a Jenway 6715 spectrometer and calibrations typically had $R^2 > 0.99$.

Uranium L_{III}-edge XAS Analysis. At the end of the bioreduction and reoxidation experiments, moist sediment pellets were obtained by centrifugation for XAS analysis. The resulting wet pastes (typically 0.5 g of sediment with <50% water content) were individually mounted under appropriate atmospheric conditions in airtight XAS sample cells. The samples were then stored under Ar at -80 °C until XAS analysis which was conducted at the Diamond Lightsource, U.K. Here, U L_{III}-edge spectra were collected at room temperature on beamline B18 in fluorescence mode using a 9-element Ge
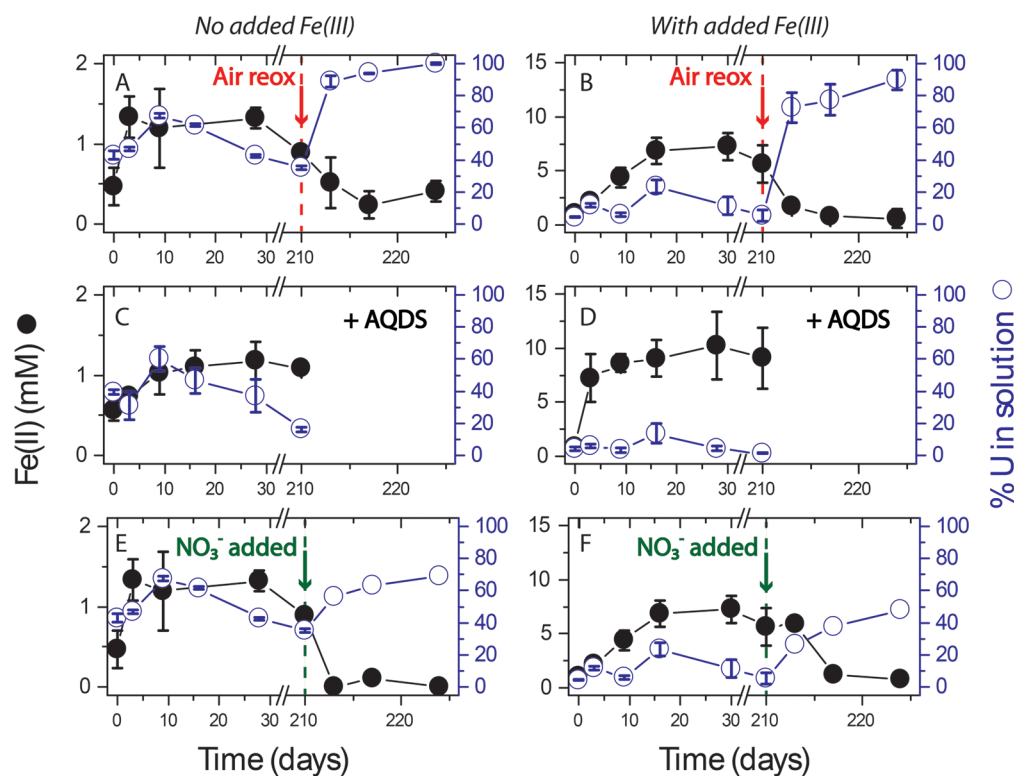
Figure 1. The 0.5 N HCl extractable Fe(II) concentration (mM) (●) and total $U_{(aq)}$ (expressed as % of the added U(VI)) (O). Systems: (A) no added Fe(III) reduction with air reoxidation after 210 days; (B) with added Fe(III) reduction and air reoxidation after 210 days; (C) no added Fe(III) reduction + AQDS; (D) with added Fe(III) reduction + AQDS; (E) with added Fe(III) reduction and nitrate reoxidation after 210 days; and (F) with added Fe(III) reduction and air reoxidation after 210 days. Error bars are 1σ of triplicate results (where not shown, errors are within the size of the symbol). Dashed lines indicate the start of reoxidation experiments; red for air and green for nitrate treatments (nitrate reoxidations were run as single experiments).

detector.[28] Standard spectra were also collected in transmission mode for U(VI) (as schoepite) and U(IV) (as uraninite). Energy calibration was completed by parallel measurement of a Y foil. Spectra were merged using ATHENA[29] and linear combination fitting between an oxic, U(VI) bearing sample (the oxic *with added Fe(III)* XANES spectrum) and a reduced, predominantly U(IV) bearing sample (the *with added Fe(III) + AQDS* reduced XANES spectrum) was undertaken to gain insight into the relative extent of reduction of U(VI) to U(IV) and using ATHENA[29,30] (SI). Latterly, background subtraction, data normalization, and fitting of the EXAFS spectra were performed using ATHENA and ARTEMIS[29] and comparison with spectra from the relevant literature. Shells were only included in the final fit if they improved the goodness of fit (R) by >5% and were statistically significant as assessed by the reduced X^2 test.

16S rRNA Gene Amplicon Pyrosequencing and Data Analysis. Bacterial community structure was examined in the bulk Buxton sediment and also in the *no added Fe(III)*, and *with added Fe(III)* microcosms at incubation end points. Samples from the subsequent nitrate reoxidation experiments were also characterized after 14 days of reoxidation. DNA was isolated from ca. 0.2 g of sediment using the MoBio PowerSoil DNA Isolation Kit (MoBio Laboratories, Inc., Carlsbad, CA, U.S.A.). PCR for amplicon pyrosequencing was performed using tagged fusion bacterial primers 27F[31] and 338R,[32] targeting the V1−V2 hypervariable region of the bacterial 16S rRNA gene (SI). The pyrosequencing run was performed at The University of Manchester sequencing facility, using a Roche 454 Life Sciences

GS Junior system. The 454 pyrosequencing reads were analyzed using Qiime 1.6.0 release,[33] and denoising and chimera removal was performed in Qiime during Operational Taxonomic Unit (OTU) picking (at 97% sequence similarity) with usearch.[34] Taxonomic classification of all reads was performed in Qiime using the Ribosomal Database Project (RDP) at 80% confidence threshold,[35] while the closest GenBank match for the OTUs that contained the highest number of reads (the representative sequence for each OTU was used) was identified by Blastn nucleotide search. In addition, rarefaction curves were computed by Qiime. The raw 38 623 pyrosequencing reads of this study have been deposited in the NCBI Sequence Read Archive (SRA) under accession number SRP036830 (BioProject ID: PRJNA236650).

■ RESULTS AND DISCUSSION

Sediment Bioreduction Experiments. To explore the biogeochemistry of uranium under anoxic conditions at pH 10−10.5, microcosms were established using calcite dominated sediment and groundwater (SI Table S1 and ref 18 for mineralogical information) from a high pH lime workings site in the U.K. and similar to past work.[18] There was a progression of microbial redox processes in both the *no added Fe(III)* and *with added Fe(III)* microcosms which were maintained at pH 10−10.5 (Figure 1A,B). For the *no added Fe(III)* system, nitrate, which was present at low but measurable concentrations (53 μM), dropped rapidly after incubation, and was below the limit of detection after 3 days. This was followed by the subsequent ingrowth of 0.5 N HCl extractable Fe(II) from day

3 onward due to microbially mediated Fe(III) reduction. In addition, the E_h fell from $+69 \pm 10$ mV at the start of the experiment, to -193 ± 7 mV after 28 days (SI Figure S1). Over longer-term 210 day incubations, the sulfate concentration remained constant (74 ± 1 μM), confirming that significant microbial sulfate reduction did not occur at pH $10-10.5$, similar to observations in other alkaline, anoxic experiments.[17,18] In the *with added Fe(III)* experiments, rapid development of reducing conditions also occurred, with nitrate removal and Fe(II) ingrowth occurring by day 3 and a drop in E_h from $+60 \pm 6$ mV at $t = 0$ to -170 ± 17 mV observed by 28 days (SI Figure S1). This was accompanied by significant levels of Fe(III) reduction with development of black sediment coloration and with 0.5 N HCl extractable Fe(II) at 7.3 ± 1.2 mM (Figure 1B). By 210 days, there was a decrease in 0.5 N extractable Fe(II) and clear formation of a black magnetic mineral phase consistent with the formation of (bio)magnetite as previously documented under parallel high pH conditions.[18] Again, sulfate concentrations remained constant throughout incubation, confirming that no sulfate reduction occurred at pH $10-10.5$. In the *no added Fe(III) + AQDS* experiment, AQDS addition had little overall impact on the rate of Fe(III)-reduction (Figure 1C) while for the *with added Fe(III) + AQDS* experiment, there was an increased rate of Fe(III)-reduction compared to the system without the electron shuttle. The total extent of Fe(III) reduction was however essentially the same (within error) in these systems (Figure 1B,D).

Uranium Fate during Bioreduction—*No Added Fe(III)*. To investigate uranium behavior in the Buxton sediment microcosms, U(VI) was incubated with a range of sediment treatments and controls. In the *no added Fe(III)* microcosms, $45.5 \pm 2.8\%$ of the added U(VI) remained in solution after 1 h (Figure 1A). The concentration of uranium in solution then fluctuated over the first fortnight and thereafter trended downward to a final value of $35.1 \pm 1.3\%$ of the original added concentration by day 210 (Figure 1A). In addition, a spectrophotometric U(VI) assay was run on early-, mid-, and end-time point samples, and this indicated that soluble uranium in these experiments was predominantly U(VI). In order to explore the solid-phase speciation and behavior of uranium further in these heterogeneous systems, uranium L_{III}-edge XANES and EXAFS spectra were collected on selected samples. The reduced *no added Fe(III)* sample at 210 days showed a XANES spectrum intermediate between the oxic and reduced end-members which suggested that partial reduction of sediment-associated U(VI) had occurred (SI Figure S3). Linear combination fitting of the XANES spectra between the oxic and reduced end-members suggested an approximate 50:50% contribution from the oxic and reduced end-member spectra, respectively (SI Table S2). The corresponding EXAFS spectra for this sample were broadly consistent with this interpretation and could be best fit with approximately 60% U(VI) and 40% U(IV) content (defined by a model consisting of 1.2 O_{ax} at 1.82 Å and 4.8 O_{eq} at 2.42 Å; SI Table S3). In the *no added Fe(III) + AQDS* system, U(VI) removal from solution was similar to the experiment without AQDS, but with only $16.4 \pm 1.3\%$ of the added uranium remaining in solution after 210 days, modestly lower than in the parallel experiment without an added electron shuttle (Figure 1C). Linear combination fitting of the XANES spectra with the oxic and reduced end-members suggested an approximate 25% U(VI): 75% U(IV) mix in the sample (SI Table S2). Again, the EXAFS data were broadly consistent with this interpretation, and the spectra could be modeled with a

best fit of approximately 35% U(VI) and 65% U(IV) (0.7 O_{ax} at 1.75 Å, 8 O_{eq} at 2.34 Å; Figure 2, SI Table S3). Interestingly, in
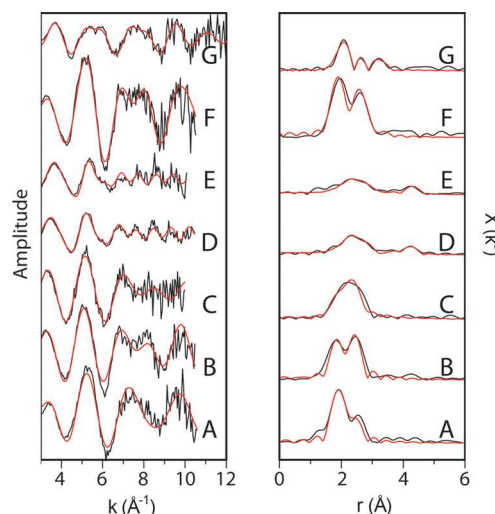
Figure 2. The k^3 weighted ^{238}U $L_{(III)}$ edge EXAFS spectra (left) and corresponding phase corrected k^3 Fourier transform (right) for bioreduction systems at experimental end-points: (A) no added Fe(III) oxic sediment; (B) no added Fe(III) reduction; (C) no added Fe(III) + AQDS reduction; (D) with added Fe(III) reduction; (E) with added Fe(III) + AQDS reduction; (F) no added Fe(III) and subsequent nitrate reoxidation; and (G) with added Fe(III) and subsequent nitrate reoxidation. Black lines are the experimental data and red lines are the best-fit models (SI Table S3).

both the *no added Fe(III)*, and *no added Fe(III) + AQDS* experiments, the U(IV) component of the spectrum did not display evidence for the characteristic uraninite, U—O—U backscatter at 3.8 Å (Figure 2B,C). The absence of this distinctive feature suggests that a non-uraninite U(IV) phase may dominate in this high carbonate, pH $10-10.5$ system.

Uranium Fate during Bioreduction—*with Added Fe(III)*. In the microbially active *with added Fe(III)* microcosms, almost complete ($95.1 \pm 0.2\%$) sorption of U(VI) to the sediment occurred by 1 h. Thereafter, during bioreduction, the uranium concentrations in solution were variable for the first fortnight and then remained low over the remainder of the experiment, with the biogeochemical changes in the system having little effect on the U-solubility (Figure 1B). Initial sorption at pH $10-10.5$ was enhanced compared to the *no added Fe(III)* system and was likely dominated by reaction of U(VI) with ferrihydrite.[36] In the *with added Fe(III) + AQDS* system, the addition of the soluble electron shuttle had little effect on uranium solubility which showed again showed strong sorption (again presumably to ferrihydrite) in the first hour (Figure 1D). Again, solid phase U-speciation was examined using XAS on select samples. In the *with added Fe(III)* system at 210 days, the XANES spectra showed reduction to U(IV) (SI Figure S3) with linear combination fitting suggesting that U(IV) was dominant in the sample (85% U(IV); SI Table S2). The corresponding EXAFS spectrum was consistent with this, and was dominated by a U(IV) like coordination environment with the model fitting 7 O backscatterers at 2.32 Å. In addition, fitting of an additional shell of 1.2 U backscatters at 3.83 Å (reflecting a potential contribution from the U—O—U coordination at 3.87 Å seen in nanoparticulate uraninite[10,37]) improved the fit and suggested a possible uraninite like

contribution within this complex sample (Figure 2; SI Table S3). Interestingly, in this sample the addition of C backscatterers at 2.96 Å significantly improved the fit (SI Table 3). This is consistent with this carbonate rich sample also containing a significant component of a nonuraninite U(IV) carbonate like phase.[10] In the *with added Fe(III) + AQDS* system the XANES spectrum again showed significant reduction to U(IV) and this sample was used as the reduced end member for linear combination fitting. Interestingly, the EXAFS spectrum could again be best fit with a contribution from both uraninite and non-uraninite U(IV) carbonate like phases similar to the parallel sample without AQDS addition (Figure 2, SI Table S3). Finally, a sterilized (autoclaved) *with added Fe(III)* sediment which had previously undergone significant Fe(III)-reduction producing (bio)magnetite (36% Fe(II)/Fe$_{tot}$) as the dominant end product,[18] was reacted with U(VI) under anoxic conditions for 7 days to explore pathways of abiotic versus enzymatic reduction. Here, the sterile, reduced sediment showed only modest reactivity to U(VI) with 24 ± 2% of U(VI) removed to the solid phase. Analysis of a XANES spectrum for this sample showed a U(VI) like spectrum and linear combination fitting between U(VI) and U(IV) standards showed, within error, that all of the sorbed uranium was present as U(VI) (SI Table S2). This suggested that pathways for abiotic reduction of U(VI) in these high pH, calcium carbonate/(bio)magnetite dominated systems were minimal and similar to work at ambient pH.[3,5,8] This may be due to the nature of the (bio)magnetite formed in this system, which has been shown in the absence of AQDS to have a non-stoichiometric Fe(II)/Fe(III) ratio with reduced Fe(II) compared to stoichiometric magnetite,[18] and further work on the balance between abiotic and enzymatic reduction of U(VI) at high pH is clearly warranted.

Reoxidation Experiments. A range of nitrate and air reoxidation experiments were performed to investigate the stability of uranium in the bioreduced sediments. Air reoxidation of the *no added Fe(III)* experiment showed significant reoxidation of Fe(II) to Fe(III) by 14 days with complete remobilization of uranium to solution as U(VI) (Figure 1A). Interestingly, the reoxidized sediment showed less affinity for U(VI) than the original material. This is presumably because of gross changes in solution chemistry and mineralogy brought on by bioreduction similar to previous observations.[11,38,39] For the air reoxidation of the *with added Fe(III)* sediments, again there was significant Fe(II) reoxidation and complete U(VI) remobilization by 14 days, with the reoxidized sediment showing little affinity for U(VI) in stark contrast to the original experiment where >95% removal was seen by 1 h. For these samples, oxidative remobilization of uranium was essentially complete such that XAS was not possible on the reoxidized materials.

With nitrate reoxidation, the *no added Fe(III)* system showed significant denitrification after 14 days (SI Figure S2). At this point, essentially complete Fe(II) oxidation had occurred coupled to a rise in E_h and soluble U(VI) increased from 151 μM at the start of the reoxidation to 270 μM at the end point (Figure 1E). In the *with added Fe(III)* experiment significant (93%) denitrification of the 30 mM nitrate occurred (SI Figure S2) coupled to a rise in E_h. Complete reoxidation of 0.5 N HCl extractable Fe(II) had occurred by 14 days. Remobilization of uranium to solution was significant with ca. 50% present in solution as U(VI) at 14 days, again highlighting that the reoxidized sediment had a significantly lower affinity for U(VI)

than the original material. Interestingly, the nitrate reoxidation experiments showed less remobilization of uranium to solution compared to the parallel air reoxidation experiments and XAS analysis on the sediments was possible. In the *no added Fe(III)* nitrate reoxidized system, the XANES showed essentially complete reoxidation to U(VI) (SI Table S2 and Figure S4) and the EXAFS data could be modeled as a U(VI) carbonate like species,[40] with 2 O$_{ax}$ at 1.79 Å, 6 O$_{eq}$ at 2.44 Å and 3 C at 2.96 Å, confirming essentially complete reoxidation of the sample (Figure 2; SI Table S3). In the *with added Fe(III)* system, the nitrate reoxidation XANES spectrum was a very poor fit to the U(IV) and U(VI) models, suggesting complex speciation (SI Table S2). Comparison with relevant literature showed that both the XANES and EXAFS data had similarities to a study showing uranium associations with partially reoxidized magnetite.[41] This is clearly relevant as (bio)-magnetite has been microbially reoxidized in our experiments. Assuming the work of Huber et al., 2012[41] allows sensible identification of the U-speciation in our experiments, the broad asymmetric XANES spectrum with white line broadening is taken to indicate a mixture of oxidation states in the sample[41] (SI Figure S4). Furthermore, the EXAFS spectrum for this sample was equally complex requiring several shells of backscatterers to achieve a good fit. In this complex system, we used the model of Huber et al. 2012,[41] as a framework for fitting. Refinement of this model with inclusion of only statistically significant shells showed a best fit of 0.5 O$_{ax}$ at 1.78 Å, 3 O$_{eq}$ at 2.22 Å, and 1 O$_{eq}$ at 2.48 Å, and with the axial oxygen occupancy, implying an approximate 25% U(VI) contribution (Figure 2, SI Table S3). In addition, the strong signal in the EXAFS at 3.21 Å was best fit with 3 Fe backscatterers suggesting that the uranium was in an iron rich, possibly incorporated environment in this reoxidized sediment. Overall, this sample showed a clearly different coordination environment to the other samples (Figure 2), and the fit we applied suggests a potential for U(IV), U(V) and U(VI) in a range of (distorted) coordination geometries, and with both uranyl and uranate components, in agreement with recent work on U reaction with iron oxide phases.[41−43] The fate of U in this sample was very complex and, coupled to the observation that U may become incorporated into iron oxides on biocycling, is clearly of relevance to the fate of U in intermediate level waste disposal.

Bacterial Diversity Assessed by 16S rRNA Gene Amplicon Pyrosequencing. Pyrosequencing of the unamended Buxton sediment revealed a diverse community with 10028 reads (after denoising and removal of short chimeric reads) grouped to 768 OTUs (at 97% sequence ID similarity) affiliated to 22 bacterial phyla. These were dominated by Bacteroidetes (44.2%), β-Proteobacteria (25.5%), and Firmicutes (16.6%) (Figure 3; SI Table S5). After 210 days incubation of the *no added Fe(III)* sediment, a far less diverse community was seen with 6358 reads and 239 OTUs (SI Table S5). This interpretation was supported by rarefaction curves (SI Figure S5). Sequence analyses showed that there was a clear enrichment in Firmicutes (47.1%) and Bacteriodetes (41.3%) (Figure 3). A similar streamlining of diversity was observed in the *with added Fe(III)* system after 210 days incubation, with 7504 reads and 217 OTUs, again with Firmicutes (48.8%) and Bacteriodetes (34.2%) dominating (Figure 3; SI Table S5). These community shifts may indicate that alkaline metal reduction is driven by these Gram-positive Firmicutes and Bacteriodetes bacteria. Interestingly, to date all

13553

dx.doi.org/10.1021/es5017125 | *Environ. Sci. Technol.* 2014, 48, 13549−13556
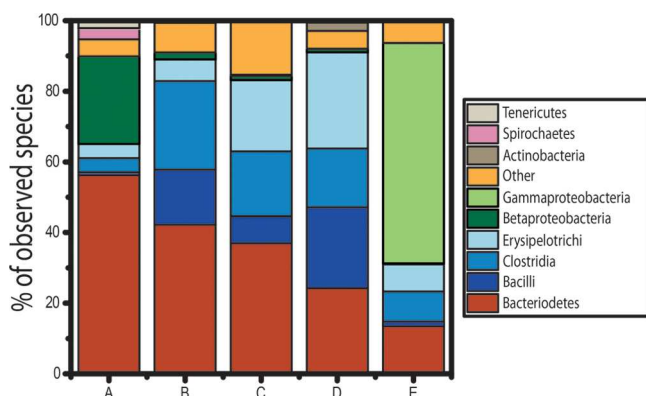
Figure 3. Bacterial phylogenetic diversity at the Phylum level for (A) bulk unamended sediment; (B) no added Fe(III) reduction; (C) with added Fe(III) reduction; (D) no added Fe(III) and subsequent nitrate reoxidation; and (E) with added Fe(III) and subsequent nitrate reoxidation. Only the phyla with more than 1% of the total number of reads are shown. Abundance at the class level is shown for Firmicutes (blue hues) and Proteobacteria (green hues).

anoxic cultures of bacteria that have been reported to reduce Fe(III) at alkaline pH also belong to the Gram-positive Firmicutes phylum and more specifically the Bacilli[44,45] and Clostridia classes.[46−50] It is noteworthy that the mechanisms of Fe(III)- and U(VI)-reduction are poorly understood in Gram-positive species that lack an outer membrane with *c*-type cytochromes that are implicated in Fe(III) and U(VI) reduction in Gram-negative cells, for example, *Geobacter* and *Shewanella* species.[51] Nevertheless, many of the dominant identified OTUs of this study were not closely affiliated to any cultured microorganisms (showing less than 90% ID similarity), but in most cases they were related closely to environmental sequences previously found in highly alkaline environments (SI Table S6). Moreover, 2−10.8% of the sequences in these three bacterial communities were closely related (99% ID similarity) to not only sequences previously detected in samples from the same site,[18] but also to uncultured bacterium clone D0488D12 (accession number GU559506) from a uranium contaminated aquifer[52] (SI Table S6).

Following the 14 day reoxidation incubation with nitrate, the microbial community of the *no added Fe(III)* treatment was further enriched in Firmicutes related sequences. Further community analysis revealed that 17.6% of the reads were affiliated (100% ID similarity) to an uncultured Erysipelotrichaceae bacterium clone 8GT0-42 (JX417293), previously detected at the same experimental site,[18] and 16.1% of the reads had 94% sequence similarity to an alkaliphilic nitrate-reducing *Bacillus* sp. JAEA No. 3-2 (AB437410) (SI Table S5). In contrast, the microbial community of the *with added Fe(III)* nitrate reoxidized sediment appeared to favor the dominance (66.1% of the population) of reads that were closely related (98% ID similarity) to *Pseudomonas peli* strain: R-20805,[53] (NR_042451) (SI Table S6), consistent with the ability to respire nitrate.

Significance. In this study, we demonstrate for the first time that an indigenous microbial community can mediate significant U(VI) reduction at pH 10−10.5 in sediments from a lime workings site despite the reported stability of U(VI) at elevated pH and mildly reducing conditions. The U(IV) which formed on bioreduction showed differences in its speciation: the *no added Fe(III)* EXAFS spectra were indicative of a non-

uraninite U(IV) phase while in ferrihydrite amended systems, the U(IV) speciation was complex with both uraninite and non-uraninite components potentially present. Interestingly, pyrosequencing revealed that the microbial ecology of the bioreducing systems was dominated by Gram-positive species, in contrast to studies examining U(VI) reduction at neutral pH where Gram-negative species often dominate.[5] Furthermore, when U(VI) was added to a pre-reduced Fe(III)-reducing sediment that had been sterilized under anoxic conditions, there was low uranium sorption and XAS confirmed that only U(VI) was present in the sediment, suggesting that enzymatic pathways for U(VI) reduction were dominant in these systems. Experiments with the addition of AQDS as an extracellular electron shuttle showed modestly enhanced U(VI)-reduction in both *no added Fe(III)* and *with added Fe(III)* experiments, again suggesting a role for extracellular electron transport in metal reduction at high pH (pH 10−10.5). Sediment reoxidation experiments showed essentially complete U(VI) remobilization after 14 days of air reoxidation in both systems. In the nitrate reoxidation experiments, less remobilization was observed, and XAS analysis revealed a complex fate for the uranium in the nitrate reoxidized sample *with added Fe(III)* with potentially U(IV), U(V) and U(VI) components in the spectrum and with a suggestion that some incorporation into this reoxidized iron oxide rich sample may be possible. In conclusion, these data highlight the importance and complexity of biogeochemical processes in controlling the long-term fate of uranium in conditions directly relevant to the geological disposal of intermediate level radioactive wastes in both the engineered barrier and the chemically disturbed, alkaline host rock environment.

■ ASSOCIATED CONTENT

S **Supporting Information**

Details of sediment and surface water composition, linear combination fitting analysis, XAS modeling, design of tagged fusion primers and PCR amplifications, E_h data for the bioreduction experiment, nitrate data from the reoxidation experiment, U L_{III} edge XANES spectra from all bioreduced and nitrate reoxidized samples, rarefaction curves, Buxton surface water composition, XANES linear combination fitting, EXAFS fitting results, pyrosequencing data processing, and phylogenetic affiliations of the most abundant bacterial OTUs identified. This material is available free of charge via the Internet at http://pubs.acs.org.

■ AUTHOR INFORMATION

Corresponding Author
*E-mail: jon.lloyd@manchester.ac.uk.
Notes
The authors declare no competing financial interest.

■ ACKNOWLEDGMENTS

■ REFERENCES

(1) Morris, K.; Law, G. T. W.; Bryan, N. D. Chapter 6. Geodisposal of Higher Activity Wastes. In *Nuclear Power and the Environment*; Harrison, R., Ed.; The Royal Society of Chemistry: London, U.K., 2011; pp 129–151.

(2) Clark, D. L.; Hobart, D. E.; Neu, M. P. Actinide carbonate complexes and their importance in actinide environmental chemistry. *Chem. Rev.* **1995**, *95* (1), 25–48.

(3) Newsome, L.; Morris, K.; Lloyd, J. R. The biogeochemistry and bioremediation of uranium and other priority radionuclides. *Chem. Geol.* **2014**, *363*, 164–184.

(4) Lovley, D. R.; Phillips, E. J. P. Bioremediation of uranium contamination with enzymatic uranium reduction. *Environ. Sci. Technol.* **1992**, *26* (11), 2228–2234.

(5) Williams, K. H.; Bargar, J. R.; Lloyd, J. R.; Lovley, D. R. Bioremediation of uranium-contaminated groundwater: a systems approach to subsurface biogeochemistry. *Curr. Opin. Biotechnol.* **2013**, *24* (3), 489–497.

(6) Anderson, R. T.; Vrionis, H. A.; Ortiz-Bernad, I.; Resch, C. T.; Long, P. E.; Dayvault, R.; Karp, K.; Marutzky, S.; Metzler, D. R.; Peacock, A.; et al. Stimulating the in situ activity of *Geobacter* species to remove uranium from the groundwater of a uranium-contaminated aquifer. *Appl. Environ. Microbiol.* **2003**, *69* (10), 5884–5891.

(7) N'Guessan, A. L.; Vrionis, H. A.; Resch, C. T.; Long, P. E.; Lovley, D. R. Sustained removal of uranium from contaminated groundwater following stimulation of dissimilatory metal reduction. *Environ. Sci. Technol.* **2008**, *42* (8), 2999–3004.

(8) Bargar, J. R.; Williams, K. H.; Campbell, K. M.; Long, P. E.; Stubbs, J. E.; Suvorova, E. I.; Lezama-Pacheco, J. S.; Alessi, D. S.; Stylo, M.; Webb, S. M.; et al. Uranium redox transition pathways in acetate-amended sediments. *Proc. Natl. Acad. Sci. U. S. A.* **2013**, *110* (12), 4506–4511.

(9) Bernier-Latmani, R.; Veeramani, H.; Vecchia, E. D.; Junier, P.; Lezama-Pacheco, J. S.; Suvorova, E. I.; Sharp, J. O.; Wigginton, N. S.; Bargar, J. R. Non-uraninite products of microbial U(VI) reduction. *Environ. Sci. Technol.* **2010**, *44* (24), 9456–9462.

(10) Boyanov, M. I.; Fletcher, K. E.; Kwon, M. J.; Rui, X.; O'Loughlin, E. J.; Loffler, F. E.; Kemner, K. M. Solution and microbial controls on the formation of reduced U(IV) species. *Environ. Sci. Technol.* **2011**, *45*, 8336–8344.

(11) Law, G. T. W.; Geissler, A.; Burke, I. T.; Livens, F. R.; Lloyd, J. R.; McBeth, J. M.; Morris, K. Uranium redox cycling in sediment and biomineral systems. *Geomicrobiol. J.* **2011**, *28* (5–6), 497–506.

(12) Campbell, K. M.; Veeramani, H.; Ulrich, K.-U.; Blue, L. Y.; Giammar, D. E.; Bernier-Latmani, R.; Stubbs, J. E.; Suvorova, E.; Yabusaki, S.; Lezama-Pacheco, J. S.; Mehta, A.; Long, P. E.; Bargar, J. R. Oxidative dissolution of biogenic uraninite in groundwater at Old Rifle, CO. *Environ. Sci. Technol.* **2011**, *45* (20), 8748–8754.

(13) Cerrato, J. M.; Barrows, C. J.; Blue, L. Y.; Lezama-Pacheco, J. S.; Bargar, J. R.; Giammar, D. E. Effect of Ca^{2+} and Zn^{2+} on UO_2 dissolution rates. *Environ. Sci. Technol.* **2012**, *46* (5), 2731–2737.

(14) Veeramani, H.; Schofield, E. J.; Sharp, J. O.; Suvorova, E. I.; Ulrich, K.-U.; Mehta, A.; Giammar, D. E.; Bargar, J. R. Effect of Mn(II) on the structure and reactivity of biogenic uraninite. *Environ. Sci. Technol.* **2009**, *43* (17), 6541–6547.

(15) Wieland, E.; Dähn, R.; Gaona, X.; Macé, N.; Tits, J. Micro- and macroscopic investigations of actinide binding in cementitious materials. In *Cement-Based Materials for Nuclear Waste Storage*; Bart, F., Cau-di-Coumes, C., Frizon, F., Lorente, S., Eds.; Springer: New York, 2013; pp 93–101.

(16) Marty, N. C. M.; Fritz, B.; Clément, A.; Michau, N. Modelling the long term alteration of the engineered bentonite barrier in an underground radioactive waste repository. *Appl. Clay Sci.* **2010**, *47* (1–2), 82–90.

(17) Rizoulis, A.; Steele, H. M.; Morris, K.; Lloyd, J. R. The potential impact of anaerobic microbial metabolism during the geological disposal of intermediate-level waste. *Mineral. Mag.* **2012**, *76* (8), 3261–3270.

(18) Williamson, A. J.; Morris, K.; Shaw, S.; Byrne, J. M.; Boothman, C.; Lloyd, J. R. Microbial reduction of Fe(III) under alkaline conditions relevant to geological disposal. *Appl. Environ. Microbiol.* **2013**, *79* (11), 3320–3326.

(19) Anderson, C.; Johnsson, A.; Moll, H.; Pedersen, K. Radionuclide geomicrobiology of the deep biosphere. *Geomicrobiol. J.* **2011**, *28* (5–6), 540–561.

(20) Behrends, T.; Krawczyk-Bärsch, E.; Arnold, T. Implementation of microbial processes in the performance assessment of spent nuclear fuel repositories. *Appl. Geochem.* **2012**, *27* (2), 453–462.

(21) Gaona, X.; Kulik, D. A.; Macé, N.; Wieland, E. Aqueous–solid solution thermodynamic model of U(VI) uptake in C—S—H phases. *Appl. Geochem.* **2012**, *27*, 81–95.

(22) Jacquot, F.; Libert, M. F.; Romero, M. A.; Besnainou, B. In vitro evaluation of microbial effects on bitumen waste form. In *Microbial Degradation Processes in Radioactive Waste Repository and in Nuclear Fuel Storage Areas*; Wolfram, J. H., Rogers, R. D., Gazso, L. G., Eds.; Springer: Netherlands, 1997; Vol 11, pp 275–283.

(23) Riekkola, R.; Sievänen, U.; Vieno, T. Controlling of disturbances due to groundwater inflow into ONKALO and the deep repository. *Work. Rep.* **2003**, *46*.

(24) Schwertmann, U.; Cornell, R. M. *Iron Oxides in the Laboratory: Preparation and Characterisation*; Wiley-VCH: Weinheim, Germany, 2000; pp 188.

(25) Lovley, D. R.; Phillips, E. J. Rapid assay for microbially reducible ferric iron in aquatic sediments. *Appl. Environ. Microbiol.* **1987**, *53* (7), 1536–1540.

(26) Johnson, D. A.; Florence, T. M. Spectrophotometric determination of uranium(VI) with 2-(5-bromo-2-pyridylazo)-5-diethylaminophenol. *Anal. Chim. Acta* **1971**, *53* (1), 73–79.

(27) Wielinga, B.; Bostick, B.; Hansel, C. M.; Rosenzweig, R. F.; Fendorf, S. Inhibition of bacterially promoted uranium reduction: Ferric (hydr)oxides as competitive electron acceptors. *Environ. Sci. Technol.* **2000**, *34* (11), 2190–2195.

(28) Dent, A. J.; Cibin, G.; Ramos, S.; Smith, A. D.; Scott, S. M.; Varandas, L.; Pearson, M. R.; Krumpa, N. A.; Jones, C. P.; Robbins, P. E. B18: A core XAS spectroscopy beamline for Diamond. *J. Phys.: Conf. Ser.* **2009**, *190*, 012039.

(29) Ravel, B.; Newville, M. ATHENA, ARTEMIS, HEPHAESTUS: Data analysis for X-ray absorption spectroscopy using IFEFFIT. *J. Synchrotron Radiat.* **2005**, *12* (4), 537–541.

(30) Law, G. T. W.; Geissler, A.; Lloyd, J. R.; Livens, F. R.; Boothman, C.; Begg, J. D. C.; Denecke, M. A.; Rothe, J.; Dardenne, K.; Burke, I. T.; et al. Geomicrobiological redox cycling of the transuranic element neptunium. *Environ. Sci. Technol.* **2010**, *44* (23), 8924–8929.

(31) Lane, D. J. 16S/23S rRNA sequencing. In *Nucleic Acid Techniques in Bacterial Systematic*; Stackebrandt, E., Goodfellow, M.; John Wiley and Sons: New York, 1991; pp 115–175.

(32) Hamady, M.; Walker, J. J.; Harris, J. K.; Gold, N. J.; Knight, R. Error-correcting barcoded primers for pyrosequencing hundreds of samples in multiplex. *Nat. Methods* **2008**, *5* (3), 235–237.

(33) Caporaso, J. G.; Kuczynski, J.; Stombaugh, J.; Bittinger, K.; Bushman, F. D.; Costello, E. K.; Fierer, N.; Pena, A. G.; Goodrich, J. K.; Gordon, J. I. QIIME allows analysis of high-throughput community sequencing data. *Nat. Methods* **2010**, *7* (5), 335–336.

(34) Edgar, R. C. Search and clustering orders of magnitude faster than BLAST. *Bioinformatics* **2010**, *26* (19), 2460–2461.

(35) Cole, J. R.; Wang, Q.; Cardenas, E.; Fish, J.; Chai, B.; Farris, R. J.; Kulam-Syed-Mohideen, A. S.; McGarrell, D. M.; Marsh, T.; Garrity, G. M.; et al. The ribosomal database project: Improved alignments and new tools for rRNA analysis. *Nucleic Acids Res.* **2009**, *37* (suppl 1), 141–145.

(36) Waite, T. D.; Davis, J. A.; Payne, T. E.; Waychunas, G. A.; Xu, N. Uranium(VI) adsorption to ferrihydrite: application of a surface complexation model. *Geochim. Cosmochim. Acta* **1994**, *58* (24), 5465–5478.

(37) Schofield, E. J.; Veeramani, H.; Sharp, J. O.; Suvorova, E.; Bernier-Latmani, R.; Mehta, A.; Stahlman, J.; Webb, S. M.; Clark, D. L.; Conradson, S. D.; Ilton, E.; Bargar, J. R. Structure of biogenic uraninite produced by *Shewanella oneidensis* strain MR-1. *Environ. Sci. Technol.* **2008**, *42* (21), 7898−7904.

(38) Moon, H. S.; Komlos, J.; Jaffé, P. R. Biogenic U(IV) oxidation by dissolved oxygen and nitrate in sediment after prolonged U(VI)/Fe(III)/SO_4^{2-} reduction. *J. Contam. Hydrol.* **2009**, *105* (1−2), 18−27.

(39) Begg, J. D. C.; Burke, I. T.; Lloyd, J. R.; Boothman, C.; Shaw, S.; Charnock, J. M.; Morris, K. Bioreduction behavior of U(VI) sorbed to sediments. *Geomicrobiol. J.* **2011**, *28* (2), 160−171.

(40) Hennig, C.; Ikeda-Ohno, A.; Emmerling, F.; Kraus, W.; Bernhard, G. Comparative investigation of the solution species $[U(CO_3)_5]^{6-}$ and the crystal structure of $Na_6[U(CO_3)_5]\cdot12H_2O$. *Dalton Trans.* **2010**, *39*, 3744−3750.

(41) Huber, F.; Schild, D.; Vitova, T.; Rothe, J.; Kirsch, R.; Schäfer, T. U(VI) removal kinetics in presence of synthetic magnetite nanoparticles. *Geochim. Cosmochim. Acta* **2012**, *96*, 154−173.

(42) Ilton, E. S.; Boily, J.-F.; Buck, E. C.; Skomusrski, F. N.; Rosso, K. M.; Cahill, C. L.; Bargar, J. R.; Felmy, A. R. Influence of the dynamical conditions on the reduction of U(VI) at the magnetite-solution interface. *Environ. Sci. Technol.* **2010**, *44*, 170−176.

(43) Marshall, T. A.; Morris, K.; Law, G. T. W.; Livens, F. R.; Mosselmans, J. F. W.; Bots, P.; Shaw, S. Incorporation of uranium into hematite during crystallisation from ferrihydrite. *Environ. Sci. Technol.* **2014**, *48* (7), 3724−3731.

(44) Ma, C.; Zhuang, L.; Zhou, S. G.; Yang, G. Q.; Yuan, Y.; Xu, R. X. Alkaline extracellular reduction: isolation and characterization of an alkaliphilic and halotolerant bacterium, *Bacillus pseudofirmus* MC02. *J. Appl. Microbiol.* **2012**, *112* (5), 883−891.

(45) Pollock, J.; Weber, K.; Lack, J.; Achenbach, L.; Mormile, M.; Coates, J. Alkaline iron(III) reduction by a novel alkaliphilic, halotolerant, *Bacillus* sp. isolated from salt flat sediments of Soap Lake. *Appl. Microbiol. Biotechnol.* **2007**, *77* (4), 927−934.

(46) Ye, Q.; Roh, Y.; Carroll, S. L.; Blair, B.; Zhou, J.; Zhang, C. L.; Fields, M. W. Alkaline anaerobic respiration: isolation and characterization of a novel alkaliphilic and metal-reducing bacterium. *Appl. Environ. Microbiol.* **2004**, *70* (9), 5595−5602.

(47) Roh, Y.; Chon, C.-M.; Moon, J.-W. Metal reduction and biomineralization by an alkaliphilic metal-reducing bacterium, *Alkaliphilus metalliredigens* (QYMF). *Geosci. J.* **2007**, *11* (4), 415−423.

(48) Zhilina, T. N.; Zavarzina, D. G.; Osipov, G. A.; Kostrikina, N. A.; Tourova, T. P. *Natronincola ferrireducens* sp. nov., and *Natronincola peptidovorans* sp. nov., new anaerobic alkaliphilic peptolytic iron-reducing bacteria isolated from soda lakes. *Microbiology* **2009**, *78* (4), 455−467.

(49) Zhilina, T.; Zavarzina, D.; Kolganova, T.; Lysenko, A.; Tourova, T. *Alkaliphilus peptidofermentans*; sp. nov., a new alkaliphilic bacterial soda lake isolate capable of peptide fermentation and Fe(III) reduction. *Microbiology* **2009**, *78* (4), 445−454.

(50) Gorlenko, V.; Tsapin, A.; Namsaraev, Z.; Teal, T.; Tourova, T.; Engler, D.; Mielke, R.; Nealson, K. *Anaerobranca californiensis* sp. nov., an anaerobic, alkalithermophilic, fermentative bacterium isolated from a hot spring on Mono Lake. *Int. J. Syst. Evol. Microbiol.* **2004**, *54* (3), 739−743.

(51) Lloyd, J. R. Microbial reduction of metals and radionuclides. *FEMS Microbiol. Rev.* **2003**, *27* (2−3), 411−425.

(52) Elifantz, H.; N'Guessan, L. A.; Mouser, P. J.; Williams, K. H.; Wilkins, M. J.; Risso, C.; Holmes, D. E.; Long, P. E.; Lovley, D. R. Expression of acetate permease-like (apl) genes in subsurface communities of *Geobacter* species under fluctuating acetate concentrations. *FEMS Microbiol. Ecol.* **2010**, *73* (3), 441−449.

(53) Vanparys, B.; Heylen, K.; Lebbe, L.; De Vos, P. *Pseudomonas peli* sp. nov. and *Pseudomonas borbori* sp. nov., isolated from a nitrifying inoculum. *Int. J. Syst. Evol. Microbiol.* **2006**, *56* (8), 1875−1881.